VOL. 10, NO. 16, SEPTEMBER 2015 ISSN 1819-6608
ARPN Journal of Engineering and Applied Sciences

www.arpnjournals.com

TOWARD AUTOMATIC COLOR-BASED ESTIMATION AND CLASSIFICATION OF BEACH SOLID WASTE BY USING DIGITAL IMAGE PROCESSING

R. Ramos, K. De Los Reyes and G. Sánchez
Faculty of Engineering, Magdalena University, Santa Marta, Colombia
E-Mail: gsanchez@unimagdalena.edu.co

ABSTRACT

Tourist beaches suffer important levels of environmental impact as a result of various factors, including human interaction. Measuring the impact of such interaction allows for the quantification of the degree of pollution in order to define environmental policies making it possible to preserve environmental levels that do not put ecosystems at risk and that guarantee a quality experience for users of beaches. Environmental quality indexes such as ICAPTU include the quantification of solid waste presence by using manual procedures. This paper proposes a method for the automatic quantification of solid waste presence based on digital image-processing techniques. In the method proposed, the image is acquired, the objects are separated, and then a set of features is extracted to be used in a k-NN classifier. Results show that the accuracy of the classifier is above 90%.

Keywords: tourist beach, solid waste, digital imaging processing.

INTRODUCTION

Tourist beaches are zones of great economic importance. The Caribbean Region, for example, is generally characterized by a strong dependence on tourism. However, demographic growth and the growing number of tourists have exacerbated the problem of pollution, a problem that has been growing for the last two decades (Gavio, 2010).

The main sources of coastal water contamination have to do with little water exchange acting as a closed basin encouraging the accumulation of contaminants (Panke and Quimby, 2000). Different studies suggest that these sources correspond to oil spills, residual water pollution, domestic solid waste, industrial pollution, and pesticides (Bocquené and Franco, 2005; Debrot *et al*., 1999; Harbone *et al*., 2001).

The category of solid waste includes elements made of plastics, nylon, polystyrene, glass, metal and paper, and organic debris (Barbosa and Ferreira da Costa, 2007). Such pollution, despite being related to natural variables, is strongly connected to human activity and generates impact on ecosystems and on the quality of the tourist experience.

A way to control pollution levels is to establish national monitoring arrangements in order to control the type, nature and acceptable level that do not affect the ecosystems. Nevertheless, there is no standard way of monitoring solid waste on beaches, so it is common to find that the nature of the methods used varies widely (Barbosa and Ferreira da Costa, 2007).

Some research work has addressed the measurement of environmental quality on tourist beaches. The proposals consider different factors to build up an index that can be measured and which reflects the state or quality index of a specific tourist beach (Botero *et al.* 2014). An example of such an index is ICATUP (Tourist Beach Environmental Quality Index), whose measurements are structured under three sub-indexes, namely: SEQI (Sanitary Environmental Quality Indicator), EEQI (Ecological Environmental Quality Indicator), and REQI (Recreational Environmental Quality Indicator).

The SEQI index was proposed based on concepts of human health risk and illness probability for beach users; thus, different parameters were defined in order to permit the quantification process, including, among others, presence of fungi in the water, fecal coliforms, hydrocarbons, organic matter, solid waste in beach sand, and others.

Traditionally, quantification of such parameters is performed manually by a set of experts that perform a visual exam on the site and register the amount and type of solid waste that is perceptible. Because of the vast extensions of beaches, the procedure is performed on predefined zones, and an estimation of total presence is obtained by extrapolating the measurements of these areas.

This work addresses the automatic quantification of solid waste present in sand, following the same principles of other automatization procedures proposed for beach application (Sánchez and Taborda, 2014). Quantification is performed in terms of the number of appearances of predefined types of elements, and not in terms of mass unit.

Automation is made by the digital image processing acquired at the site of study and by using the same methodology of defining smaller areas. Solid waste has been classified into three groups: polystyrene, wood, and others. The last category includes organic solid waste, and metal and plastic elements, which are common in

tourist areas. This classification responds to a preliminary analysis of the characteristics of the various materials thatcan be identified from digital images. Plastics, metals and organic elements have a wide variety of colors or translucent properties that make it difficult to distinguish them by means of color property information.

The method proposed estimates a set of values characteristic of the objects present in the acquired images, and then sends the information to a classifier that determines the objects' category according to their type of material. The classifier was experimentally trained with a set of images previously acquired and classified. The method proposed allows for the classification of the elements visible in a digital image with an accuracy of 90%.

MATERIALS AND METHODS

The proposed methodology begins with image acquisition. Light variations during the day can affect the color of objects; therefore, a color-correction stage is applied in order to use predefined clusters for segmentation and classification. After correction, a mathematical transformation of RGB values to CIELAB color space is applied to the acquired images. In the segmentation stage objects are separated from beach sand, and characteristic values are measured and used to classify objects according to material. Objects are classified into three groups: polystyrene, wood, and others.

Finally, the system estimates the presence percentage of each group in the image by using pixel-distance relations. A flowchart of the method proposed is shown in Figure-1.

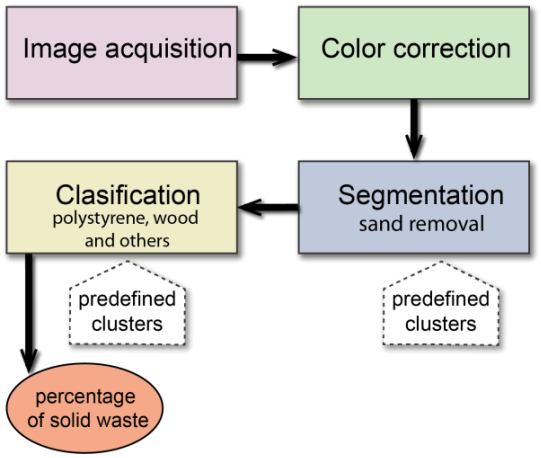

Figure-1. Methodological scheme of the method proposed.

Image acquisition

The method design is based on the use of traditional capture devices. The images were acquired with 2592x1944 pixel resolution and 300dpi, and saved in PNG format. The area of study was Rodadero bay, located at 11°12'18.9¨ N - 4°13'41.6¨ W, with a length of 1, 186 m and an approximate area of 55,683 m^2. Figure-2 shows the described site.

Figure-2. Rodadero beach on the Colombian Caribbean coast.

The specific assembly uses a standard digital camera of 16.4 mp and 25mm lens on a framework that allows to set the focal distance *df* from camera to sand. The assembly is shown in Figure-3.

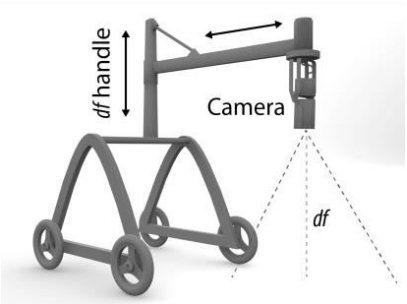

Figure-3. Acquisition assembly.

Color correction and CIELAB transformation

Color correction, noise reduction and edge detection are typical steps of the pre-processing stage in a digital image processing project.

Image color correction is necessary because the objects' position in the color space could be modified due to light variations during the day. We must bear in mind that color characteristics in an image acquired with a camera depend on three factors, namely, the physical content of the acquired scene, incident light, and the characteristics of the acquisition device; the latter two directly affect the color representation of objects. Given that the images are acquired with the same device and configuration, the method for color correction aims at diminishing incident light.

We used the Gray World algorithm, whose main idea is that for a typical image the average intensity of the red, green and blue channels should be equal. Thus, for the computation of Gray World of an image I of size FxC, it is typical to assume the green channel is kept unchanged, and

the gain for the red and blue channels is defined as follows (Lam, 2005):

$$\alpha = \frac{G_{avg}}{R_{avg}} \quad \beta = \frac{G_{avg}}{B_{avg}} \tag{1}$$

where

$$R_{avg} = \frac{1}{FC}\sum_{i=1}^{F}\sum_{j=1}^{C} I_r(i,j)$$

$$G_{avg} = \frac{1}{FC}\sum_{i=1}^{F}\sum_{j=1}^{C} I_g(i,j) \tag{2}$$

$$B_{avg} = \frac{1}{FC}\sum_{i=1}^{F}\sum_{j=1}^{C} I_b(i,j)$$

where I_r, I_g, I_b are the sub images of the red, green and blue channels, and (i,j) denote the indexes of pixel position. The pixels adjusted are:

$$\begin{aligned} \hat{I_r}(i,j) &= \alpha I_r(i,j) \\ \hat{I_g}(i,j) &= I_g(i,j) \\ \hat{I_b}(i,j) &= \beta I_b(i,j) \end{aligned} \tag{3}$$

After color correction, we performed the CIELab color space transformation through the following equations (Connolly, C. and Fleiss, 1997):

$$\begin{aligned} X &= 0.4303R + 0.3416G + 0.1784B \\ Y &= 0.2219R + 0.7068G + 0.0713B \\ Z &= 0.0202R + 0.1296G + 0.9393B \end{aligned} \tag{4}$$

$$L^* = 116 f\left(\frac{Y}{Y_0}\right) - 16$$

$$a^* = 500\left[f\left(\frac{X}{X_0}\right) - f\left(\frac{Y}{Y_0}\right)\right]$$

$$b^* = 200\left[f\left(\frac{Y}{Y_0}\right) - f\left(\frac{Z}{Z_0}\right)\right] \tag{5}$$

where

$$\begin{aligned} f(q) &= \sqrt[3]{q} \quad q > 0.008856 \\ f(q) &= 7.787q + \frac{16}{116} \quad q \le 0.008856 \end{aligned} \tag{6}$$

Where (R,G,B) represents the triestimulus in RGB color space for each pixel and (X_0, Y_0, Z_0) are defined for illuminant D65 (Valero, 2012).

Segmentation

Segmentation refers to the process of separating sand and objects within the scene. In this work, we used color-based segmentation for sand identification. Due to the significant variations of sand color because of the humidity level, the main idea was experimentally to find the sand position on color space through a set of images in order to set the threshold t_{sand} that includes the most sand color variations.

The estimation procedure initiates with grouping together the objects inside the test images. Since sand takes most of the space inside the images, the largest cluster in pixels was selected, with which the average of channels *a* and*b* is estimated from each one of the pixels (see Algorithm-1).

Algorithm-1. Estimated sand predefined centroid.

1:	function sand_centroid (*images*)
2:	for each one *images*
3:	$img_{rgb} = load()$
4:	$img_{lab} = rgbtoCIElab(img_{rgb})$
5:	$clusters = kmeans_{clusters}(img_{lab})$
6:	select *i* cluster //biggest one
7:	estimate $a_{avg}, b_{avg} \wedge L_{avg}$
8:	endfor
9:	
10:	estimate global $a_{avg}, b_{avg} and\ L_{avg}$

Sand presents variations within the color space depending on the percentage of humidity that it has. Therefore, three groups were defined for sand: dry, humid, and wet (see Figure-4).

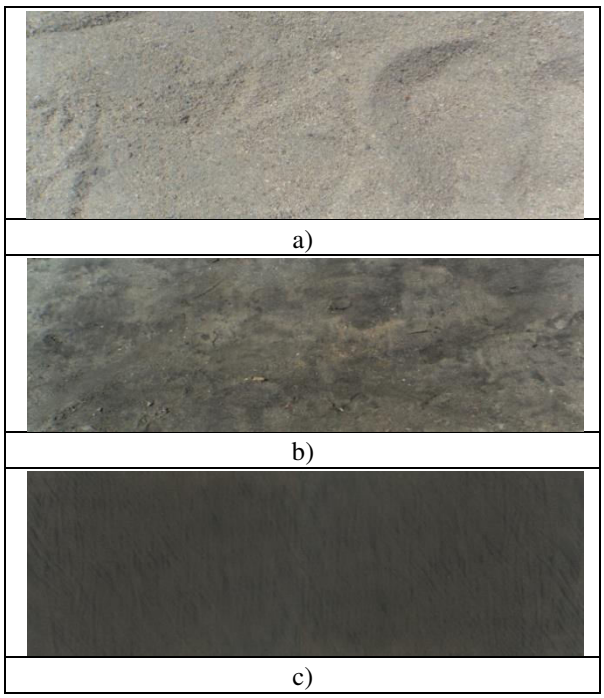

Figure-4. Color variations for sand related with the amount of humidity. a) Dry, b) humid and c) wet sand.

The procedure to eliminate sand begins by removing the pixels that are found nearby according to a metric based on Euclidean distance to the predefined centroids. Then, small regions containing isolated pixels are removed, by means of morphological operations. Figure-5 exemplifies the application of the segmentation phase.

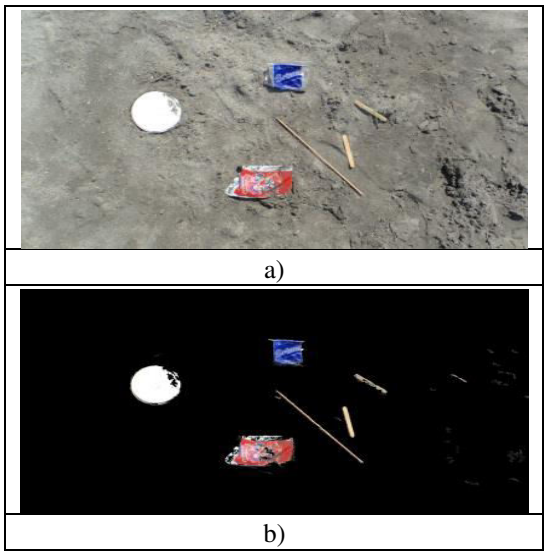

Figure-5. Example of sand removal by segmentation approach.

Once the objects have been isolated, segmentation is estimated by regions growing from a point centered on the color equal to the segmented object. This procedure based on *regions growing* allows improving segmentation in the image of objects falling under the category *others*. This is so because under this category there are objects with translucent or reflective properties such as aluminum or metal products.

K nearest neighbor classification

In order to classify the objects in the images into three defined groups, we used k-NN classification to find a set of three centroids in the color CIELab space using a set of training images.

Different classification approaches have been proposed within the academic community. The main difficulty for a practical proposal of an object classification system lies in the problems of inter-class diversity and inter-class correlation (Hou *et al*. 2014). In Tulyakov *et al*. (2008), the classification process is characterized into two groups: feature classification and classifier fusion. The first one is a classical procedure that refers to the combination of different features into a feature vector used to locate the objects into the classification domain. Classifier fusion involves the combination of the individual outputs into multiple classifiers such as Boosting (Ferreira and Figueiredo, 2012).

In this work, we adopt the feature combination technique for the classification of the objects by using a k-NN classifier. The features describing the objects are related to the color space position. The k-nearest neighbor method is one of the oldest algorithms for classical single-label learning. It is an iterative method to partition a given dataset into k clusters. Given a set of d-dimensional vectors $D = \{x_i \vee i = 1, \dots, N\}$ such, that $x_i \in R^d$ is a characteristics vector. The classical approach is initialized by selecting k points into the d-dimensional space called centroids. The learning process is done by means of iteratively assigning new data to the closest centroid and by relocating the centroids to the center of all data into the cluster.

The "closest" concept used in the learning process is typically used in the non-negative cost function:

$$\sum_{i=1}^{N} \left(\underset{j}{argmin} \|x_i - centroid_i\| \right)_2^2 \quad (7)$$

The characteristics vector for classification is defined by color features and shape features extraction.

For color features, we use the average average$a^*$and b^* components of CIELab color space of each pixel. The $L^*a^*b^*$color space is nearly proportional to human visual perception, which means that equal distances in the color space correspond to equally perceived color differences. In this color space, L^* represents lightness, and a^* and b^* are the coordinates of chromaticity. Avoiding the use of L^* for classification is addressed to make the proposed method robust under lighting variation conditions.

For shape features, we use moment invariants based on the area of the object shape representation (Hu, 1962). In this work, we use the four first Hu moment invariants. These moments are defined using a central moment definition. For a two-value image I, the p+q central moment is:

$$\mu_{p,q} = \sum_{(x,y)\in I} (x - x_c)^p (y - y_c)^q \quad (8)$$

where(x_c, y_c) is the center of I, and the coordinate (x, y) is a point in I. The four first Hu moment invariants with respect to shift, rotation and scaling are defined as:

$$\emptyset_1 = \mu_{2,0} + \mu_{0.2} \quad (9)$$

$$\emptyset_2 = (\mu_{2,0} - \mu_{0,2})^2 + 4\mu_{1,1}^2 \quad (10)$$

$$\emptyset_3 = (\mu_{3,0} - 3\mu_{1,2})^2 + (\mu_{0,3} - 3\mu_{2,1})^2 \quad (11)$$

$$\emptyset_4 = (\mu_{3,0} + \mu_{1,2})^2 + (\mu_{0,3} + \mu_{2,1})^2 \quad (12)$$

Initially, for $a^*$and b^* color features estimation, the pixels are grouped by means of a region growing procedure. The seed is set to the geometric average of the pixel set.

The classification process subdivides the color space into different size regions, where each one of the material types is located. We named each one of the regions a sub-space; thus, the sub-space size and location are defined in the training stage and depend on the training data set (see Figure-6).

Finally, once the objects have been classified, a percentage of image occupancy is calculated by using a pixel-area conversion.

To calculate this percentage, the pixel distance relation was established by means of:

$$Occupancy = \frac{af * 1cm^2}{K} \quad (13)$$

Where *Occupancy* represents the object size insq. cm, *af* equals the area of the picture in pixels, and K is the number of pixels in a sq. cm by taking into account the distance df of the acquisition mechanism.

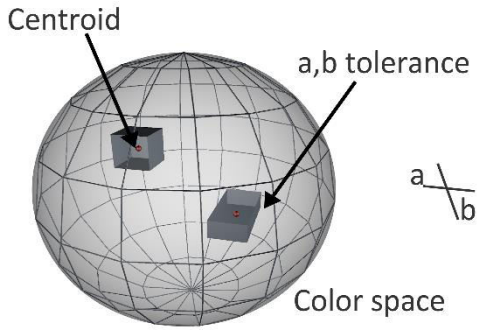

Figure-6. Subspaces defined for centroids and a^*b^* tolerance for color classification.

RESULTS AND DISCUSSIONS

To determine the tolerance threshold for the segmentation of the sand, a set of 50 training images was defined to estimate the average position of the sand. Table-1 shows the values and statistical averages for the training set. Table-2 shows the omission and commission errors for the process of sand segmentation.

Table-1. Sand color feature measure of the training set.

Feature	Sand	
	Min	Max
a*	-4	3
b*	-15	3
Standard deviation	1.018	2.076

Table-2. Results of the segmentation stage.

Sand segmentation	
Omission Error	0.00058544
Commission Error	0.07851396

Some graphic examples of image processing results can be seen on Figure-7. The sand removal procedure is applied to the original image (Figure-7a-c) to separate the group of objects (see Figure-7b-d).

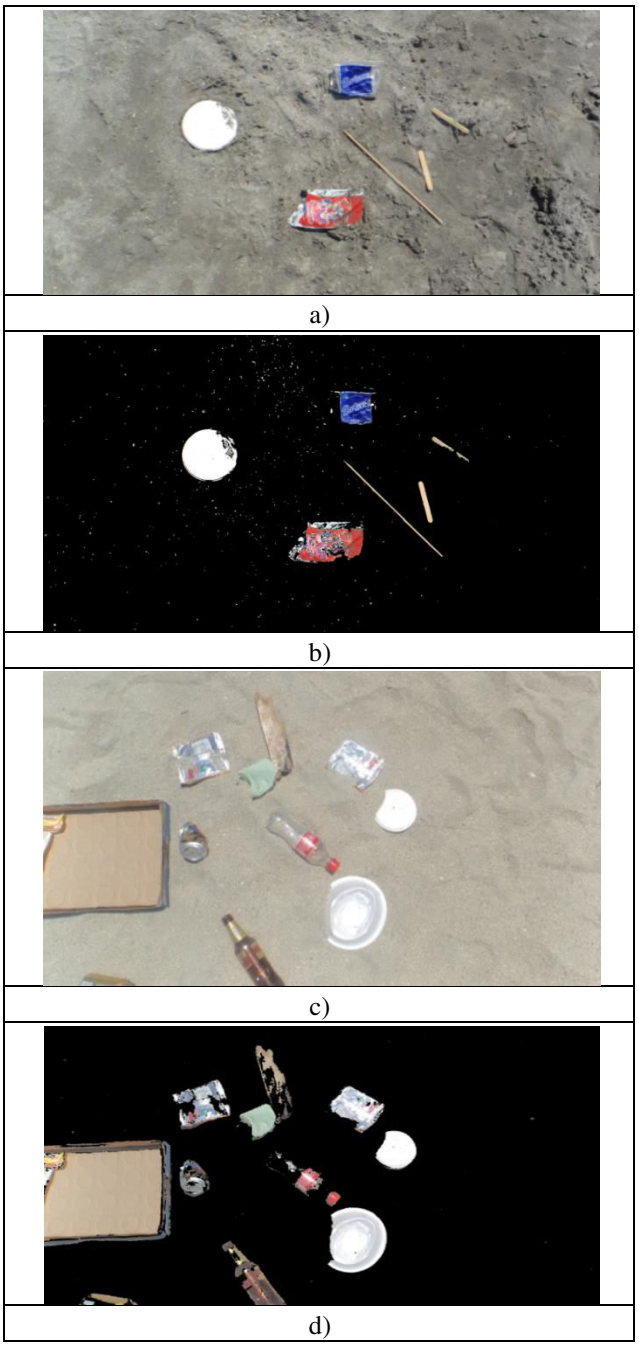

Figure-7. Sand segmentation on real images.

Once the objects have been separated, they are sent to the classifier. Table-3 shows the results of classifying 120 images by means of a confusion matrix.

Table-3. Confusion matrix for the classification.

	Polystyrene	Wood	Others
polystyrene	43	0	2
wood	0	42	6
others	0	5	22

Final results of image processing are shown on Figure-8.

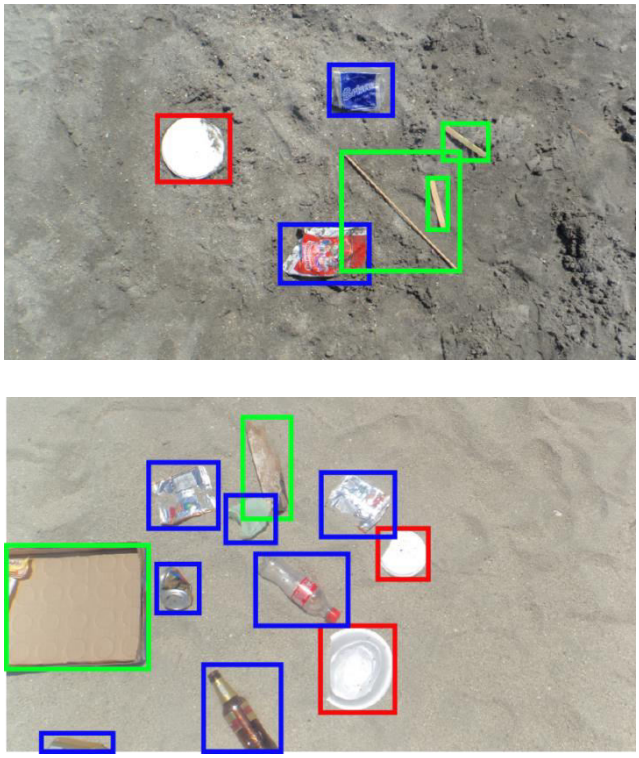

Figure-8. Example of objects classification results.

Occlusion is the main obstacle for object classification. Occlusions may be present in several forms. Occlusion among objects emerges when several objects are juxtaposed. Occlusion due to partial sand presence over objects prevents adequate classification and alters the estimation accuracy of the occupied area. Additional obstacles are related to the minimum size of objects that can be classified. Essentially, this depends on image size and resolution. Translucent objects prevent adequate segmentation, because part of the object area is removed during the sand segmentation stage.

Future work shall be focused on widening the features that may be measured in a practical way, and on light limitations which may improve classifier accuracy. Similarly, another promising path is the improvement of the acquisition device, so that images can be acquired with automatic variations of position and resolution.

REFERENCES

Barbosa M. and Ferreira da Costa M. 2007. Visual diagnosis of solid waste contamination of a tourist beach: Pernambuco, Brazil, Waste Management. 27(6): 833-839, ISSN 0956-053X.

Bocquené G. and Franco A. 2005. Pesticide contamination of the coastline of Martinique. Marine Pollution Bulletin. 51: 612-619.

Botero C., Pereira C., Tosic and M. Manjarrez G. 2014. Design of an index for monitoring the environmental quality of tourist beaches from a holistic approach, Ocean and Coastal Management, Available online 15 August 2014, ISSN 0964-5691.

Connolly C. and Fleiss T. 1997. A study of efficiency and accuracy in the transformation from RGB to CIELAB color space, Image Processing. 6(7): 1046 -1048.

Debrot A.O., Tiel A.B. and Bradshaw J.E. 1999. Beach debris in Curaçao. Marine Pollution Bulletin vol. 38, pp. 795-801.

Ferreira A. and Figueiredo M. 2012. Boosting Algorithms: A Review of Methods, Theory, and Applications. Ensemble Machine Learning. pp. 35-85, Springer, New York, USA.

Gavio B., Palmer-Cantillo S. and Mancera J. 2010. Historical analysis (2000-2005) of the coastal water quality in San Andrés Island, Sea Flower Biosphere Reserve, Caribbean Colombia, Marine Pollution Bulletin. 60(7): 1018-1030.

Hou J., Xue E., Xia Q. and Qi N. 2014. Evaluating classifier combination in object classification. Pattern Analysis and Applications. 17(1): 1-18.

Hu M. 1962. Visual pattern recognition by moment invariants, Information Theory, IRE Transactions on. 8(2): 179-187.

Lam E.Y. 2005. Combining gray world and retinex theory for automatic white balance in digital photography, Consumer Electronics. Proceedings of the Ninth International Symposium on. pp. 134, 139, 14-16 June.

Panke M. and Quimby S. 2000. Pesticides. Caribbean Currents. 8(3): 1-5.

Harborne A.R., Afzal D.C. and Andrews M.J. 2001. Honduras: Caribbean coast. Marine Pollution Bulletin. 42(12): 1221-1235.

Sanchez G. and Taborda J. 2014. Estimación automática de la medida de ocupación de playas mediante procesamiento de imágenes digitales. Tecno Lógicas. 17(33): 21-29. ISSN: 0123-7799.

Tulyakov S, Jaeger S, Govindaraju V. andDoermannD. 2008. Review of classifier combination methods. Machine Learning in Document Analysis and Recognition. 90(1): 361-386. Springer, Berlin, Hiedelberg.

Valero A. 2012. Principios del color y holopintura. Alicante: Editorial ClubUniversitario. 1 edición. ISBN 9788499483481.